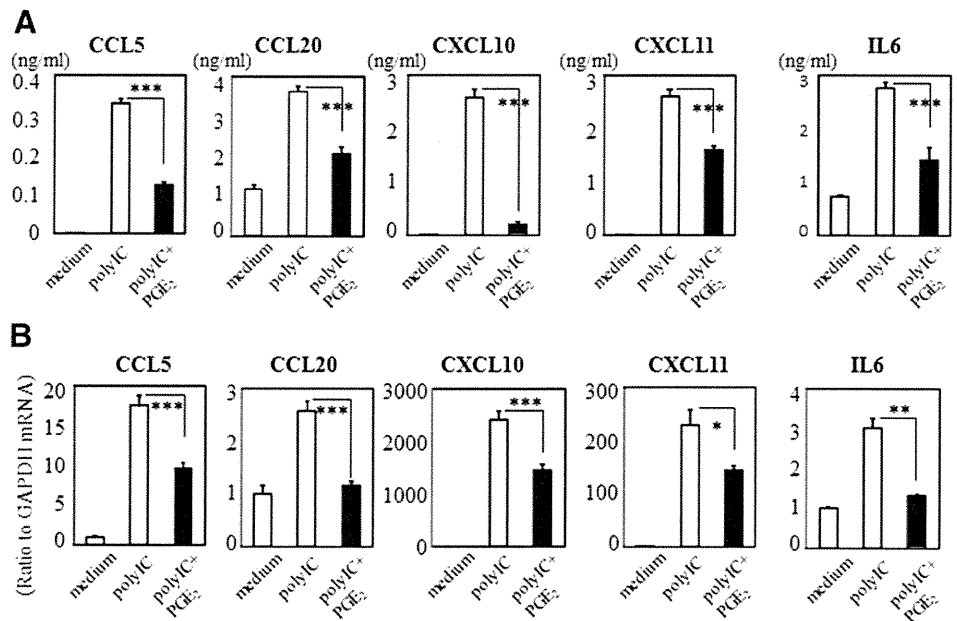


FIGURE 1. A, Suppression of the production of CCL5, CCL20, CXCL10, CXCL11, and IL-6 by PGE₂. HCLE were exposed to 10 μg/mL poly I:C and 100 μg/mL PGE₂ for 24 hours. Data are representative of 3 separate experiments and are given as the mean ± SEM from one experiment carried out in 6 wells per group. B, Suppression of mRNA expression of CCL5, CCL20, CXCL10, CXCL11, and IL-6 by PGE₂. HCLE were exposed to 10 μg/mL poly I:C and 100 μg/mL PGE₂ for 6 hours. The quantification data were normalized to the expression of the housekeeping gene GAPDH. The y axis shows the increase in specific mRNA over unstimulated samples. Data are representative of 3 separate experiments and are given as the mean ± SEM from one experiment carried out in 6 wells per group (**P* < 0.05, ***P* < 0.005, ****P* < 0.0005).



lengths were obtained for EP2 (683 bp), EP3 (622 bp), and EP4 (956 bp) (Fig. 2), but not for EP1 (723 bp) (data not shown), from HCLE and *in vivo* human corneal epithelial cells, suggesting that the human corneal epithelium expresses EP2, EP3, and EP4 mRNAs. To confirm the specificity for the detection of EP2-, EP3-, and EP4 mRNA, we isolated and sequenced the PCR products. The obtained sequences were identical to the human EP2-, EP3-, and EP4 cDNA sequences. Moreover, we could detect EP2, EP3 and EP4 proteins using immunoblotting (see **Figure, Supplemental Digital Content 1**, <http://links.lww.com/ICO/A42>).

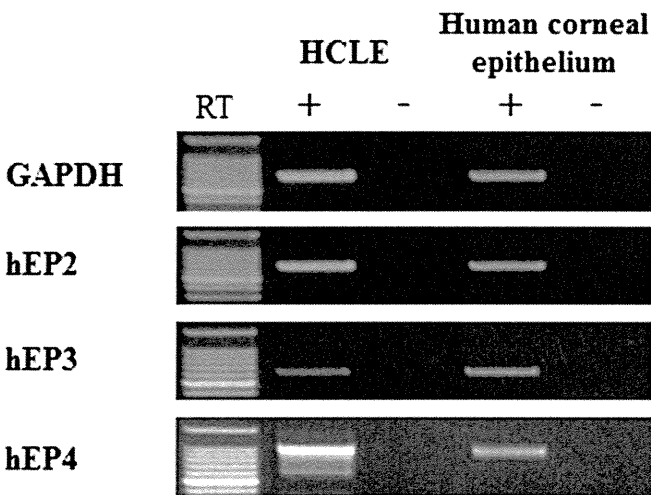


FIGURE 2. mRNA expression of the PGE₂ receptors EP2, EP3, and EP4. RT-PCR assay of the expression of PGE₂ receptor EP2, EP3, and EP4-specific mRNA in HCLE and human corneal epithelium. RT identifies data that were obtained without reverse transcription (controls).

EP2 and EP3, but not EP4 Agonists Downregulated the Production of Cytokines Induced by Poly I:C Stimulation

Using the EP2, EP3, and EP4 agonists, ONO-AE-259, ONO-AE-248, and ONO-AE-329, respectively, we also examined which PGE₂ receptor(s) contributed to their polyI:C-induced downregulation. HCLE were exposed to 10 μg/mL polyI:C and 10 μg/mL of the EP2, EP3, or EP4 agonist for 24 hours (ELISA) or 6 hours (quantitative RT-PCR). ELISA showed that the EP2 agonist significantly suppressed the polyI:C-induced production of CCL5, CXCL10, and CXCL11 (all, *P* < 0.0005) but not of CCL20 and IL-6, and that the EP3 agonist significantly suppressed the production of CCL5, CCL20, CXCL10, CXCL11, and IL-6 (all, *P* < 0.0005). However, the EP4 agonist failed to suppress the cytokine production induced by polyI:C stimulation (Fig. 3). Quantitative RT-PCR confirmed that the EP2 agonist significantly downregulated the mRNA expression of CCL5, CXCL10, and CXCL11 (respectively, *P* < 0.005, *P* < 0.0005 and *P* < 0.05), but not of CCL20 and IL-6, and that the EP3 agonist significantly downregulated the mRNA expression of all examined cytokines (CCL5, *P* < 0.05; CCL20, *P* < 0.005; CXCL10, *P* < 0.0005; CXCL11, *P* < 0.0005; and IL-6, *P* < 0.005) (Fig. 4). Thus, our results show that PGE₂ attenuated the mRNA expression and production of CCL5, CXCL10, and CXCL11 via both EP2 and EP3, and that the CCL20 and IL-6 mRNA expression and production were attenuated only by EP3 in human corneal epithelial cells.

DISCUSSION

Lipid mediators like PGE₂ regulate immune and inflammatory responses by modulating the production of cytokines and chemokines.¹¹ In macrophages, PGE₂ suppressed the proinflammatory gene expression induced by LPS,

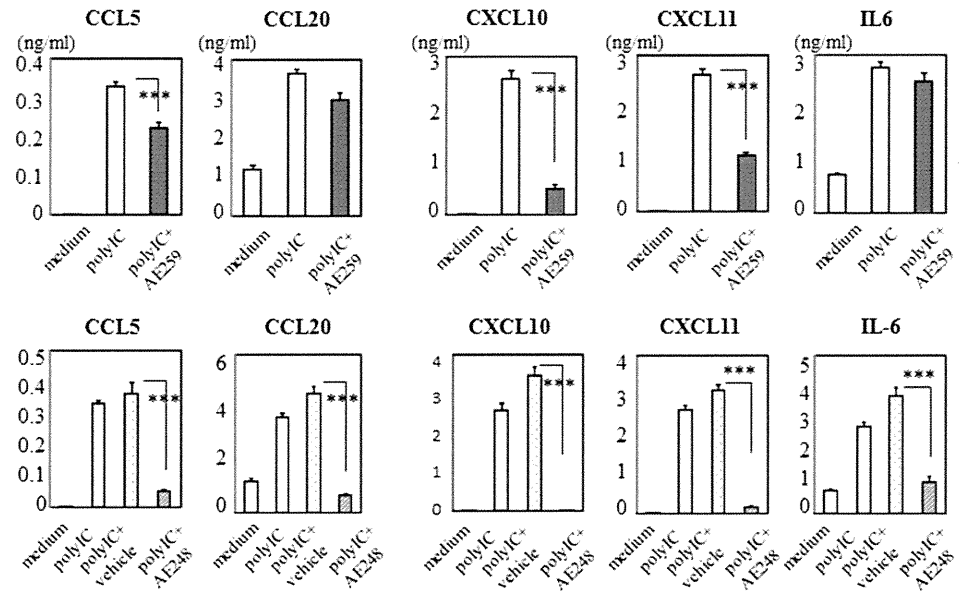
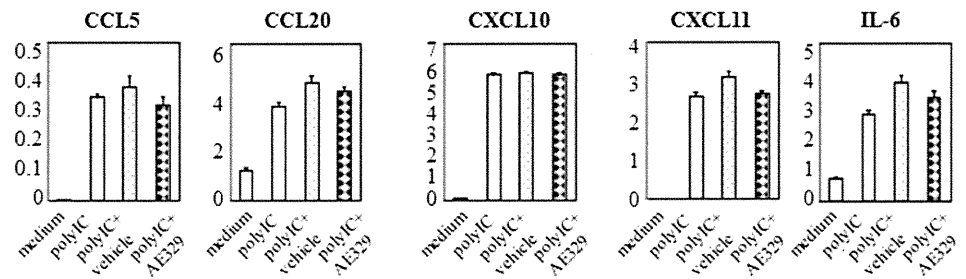


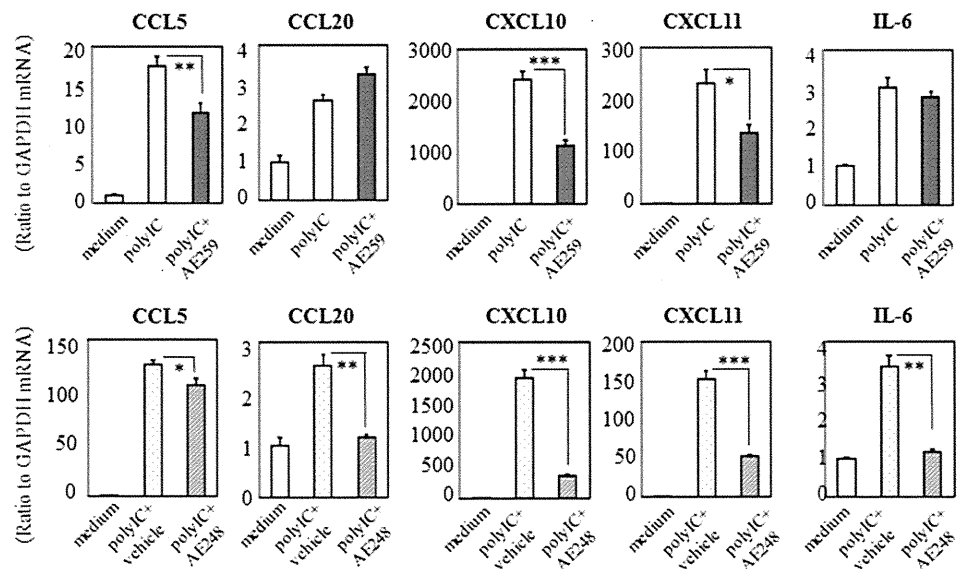
FIGURE 3. Effect of the PGE₂ receptors EP2, EP3, and EP4 on poly I:C-induced cytokine production. HCLE were exposed to 10 μg/mL poly I:C and 10 μg/mL EP2, EP3, or EP4 agonist for 24 hours. Data are representative of 3 separate experiments and are given as the mean ± SEM from one experiment carried out in 6 wells per group (***P* < 0.0005).



including macrophage inflammatory protein (MIP)-1α, MIP-1β, CCL5, CXCL10, and IL-8.⁹ Here we document that PGE₂ modulates the expression and production of poly I:C-induced proinflammatory genes in not only human conjunctival epithelial cells but also corneal epithelial cells. It exerted an inhibitory effect on poly I:C-induced CCL5,

CCL20, CXCL10, CXCL11, and IL-6 mRNAs (respectively, *P* < 0.0005, *P* < 0.0005, *P* < 0.0005, *P* < 0.05 and *P* < 0.005) and on protein production in HCLE (all, *P* < 0.0005). PGE₂ exerts its biological actions by binding to EP located primarily on the plasma membrane. We confirmed the presence of the PGE₂ receptor subtypes, EP2,

FIGURE 4. Effect of the PGE₂ receptors EP2 and EP3 on the poly I:C-induced mRNA expression of cytokines: HCLE were exposed to 10 μg/mL poly I:C and 10 μg/mL EP2 or EP3 agonist for 6 hours. The quantification data were normalized to the expression of the housekeeping gene *GAPDH*. The y axis shows the increase in specific mRNA over unstimulated samples. Data are representative of 3 separate experiments and are given as the mean ± SEM from one experiment carried out in 6 wells per group (**P* < 0.05, ***P* < 0.005, ****P* < 0.0005).



EP3, and EP4, in human corneal epithelial cells. Stimulation with either EP2- or EP3-specific agonists had a suppressive effect on polyI:C-induced CCL5, CXCL10, and CXCL11 production (both EP2- and EP3-specific agonists: all, $P < 0.0005$), but only the EP3-specific agonist had a suppressive effect on the production of CCL20 and IL-6 (both, $P < 0.0005$).

Stimulation with PGE₂ exhibits immunosuppressive effects in various cell types including macrophages and dendritic cells via EP2 and/or EP4.^{9–11} This phenomenon is explicable by the elevation of intracellular cyclic adenosine monophosphate (cAMP) via the activation of adenylylase.^{9,10} Although PGE₂ acts on EP2 and EP4 and activates adenylylase, resulting in the elevation of intracellular cAMP, its action on EP3 suppresses adenylylase, resulting in a decrease in intracellular cAMP. In human conjunctival and corneal epithelial cells, both EP2 and EP3 contribute to the immunosuppressive effect against polyI:C stimulation; therefore, the suppressive effect cannot be explained by the elevation of intracellular cAMP. The precise molecular mechanisms underlying the immunosuppressive effects of PGE₂ in epithelial cells remain to be elucidated.

Release of PGE₂ is associated with ocular inflammation, but the exact role in inflammation has not been identified, rather PGE₂ might have been considered as inflammation-related molecules in the cornea. In this study, it is evident that PGE₂ could contribute to suppressing the production of various cytokines and chemokines in the ocular surface. Elsewhere we reported that PGE₂ acts as a ligand for EP3 in conjunctival epithelial cells and that it downregulates the progression of murine experimental allergic conjunctivitis,⁷ suggesting the possibility of the PGE₂ and EP3 selective agonists as antiinflammatory drugs.

In summary, our results suggest that PGE₂ and its receptors in ocular surface (conjunctival and corneal) epithelium contribute to the regulation of ocular surface inflammation.

ACKNOWLEDGEMENTS

We thank Chikako Endo for technical assistance.

REFERENCES

1. Matsuoka T, Narumiya S. Prostaglandin receptor signaling in disease. *ScientificWorldJournal*. 2007;7:1329–1347.
2. Alexopoulou L, Holt AC, Medzhitov R, et al. Recognition of double-stranded RNA and activation of NF-kappaB by Toll-like receptor 3. *Nature*. 2001;413:732–738.
3. Ueta M, Kinoshita S. Ocular surface inflammation mediated by innate immunity. *Eye Contact Lens*. 2010;36:269–281.
4. Ueta M, Mizushima K, Yokoi N, et al. Gene-expression analysis of polyI:C-stimulated primary human conjunctival epithelial cells. *Br J Ophthalmol*. 2010;94:1528–1532.
5. Kumar A, Zhang J, Yu FS. Toll-like receptor 3 agonist poly(I:C)-induced antiviral response in human corneal epithelial cells. *Immunology*. 2006;117:11–21.
6. Ueta M, Kawai T, Yokoi N, et al. Contribution of IPS-1 to polyI:C-induced cytokine production in conjunctival epithelial cells. *Biochem Biophys Res Commun*. 2011;404:419–423.
7. Ueta M, Matsuoka T, Narumiya S, et al. Prostaglandin E receptor subtype EP3 in conjunctival epithelium regulates late-phase reaction of experimental allergic conjunctivitis. *J Allergy Clin Immunol*. 2009;123:466–471.
8. Ueta M, Matsuoka T, Yokoi N, et al. Prostaglandin E2 suppresses polyinosine-polycytidylic acid (polyI:C)-stimulated cytokine production via prostaglandin E2 receptor (EP) 2 and 3 in human conjunctival epithelial cells. *Br J Ophthalmol*. 2011;95:859–863.
9. Takayama K, Garcia-Cardena G, Sukhova GK, et al. Prostaglandin E2 suppresses chemokine production in human macrophages through the EP4 receptor. *J Biol Chem*. 2002;277:44147–44154.
10. Xu XJ, Reichner JS, Mastrofrancesco B, et al. Prostaglandin E2 suppresses lipopolysaccharide-stimulated IFN-beta production. *J Immunol*. 2008;180:2125–2131.
11. Shiraishi H, Yoshida H, Saeki K, et al. Prostaglandin E2 is a major soluble factor produced by stromal cells for preventing inflammatory cytokine production from dendritic cells. *Int Immunol*. 2008;20:1219–1229.
12. Ueta M, Hamuro J, Kiyono H, et al. Triggering of TLR3 by polyI:C in human corneal epithelial cells to induce inflammatory cytokines. *Biochem Biophys Res Commun*. 2005;331:285–294.
13. Ueta M, Kinoshita S. Innate immunity of the ocular surface. *Brain Res Bull*. 2010;81:219–228.
14. Ueta M, Sotozono C, Nakano M, et al. Association between prostaglandin E receptor 3 polymorphisms and Stevens-Johnson syndrome identified by means of a genome-wide association study. *J Allergy Clin Immunol*. 2010;126:1218–1225. e10.

Epistatic interaction between Toll-like receptor 3 (TLR3) and prostaglandin E receptor 3 (PTGER3) genes

To the Editor:

We previously reported that conjunctival eosinophilic infiltration in murine experimental allergic conjunctivitis (EAC) was significantly less marked in Toll-like receptor 3 gene (*TLR3*) knockout (KO) mice¹ and significantly more marked in prostaglandin E receptor 3 (EP3) gene (*PTGER3*) KO mice than in wild-type mice.² Considering the opposite roles of TLR3 and EP3 in allergic conjunctivitis, we speculate the possibility of unknown functional interaction between TLR3 and EP3.

Intriguingly, we have also reported that Stevens-Johnson syndrome (SJS)/toxic epidermal necrolysis (TEN) accompanied by severe ocular surface complications was associated with *TLR3* gene polymorphisms³ and *PTGER3* polymorphisms.⁴ SJS is an acute inflammatory vesiculobullous reaction of the skin and mucosa, often including the ocular surface,⁵ and TEN occurs with its progression. SJS/TEN with ocular surface complications often result in severe and definitive sequelae, such as vision loss (see Fig E1 in this article's Online Repository at www.jacionline.org).⁶

For the past decade, single nucleotide polymorphisms (SNPs) have been widely used as genetic markers for identifying human disease-susceptibility genes. However, it has become apparent that gene-gene interactions should be considered in addition to major single-locus effects.⁷ In particular, nonadditive (epistatic) models for some complex diseases fit to actual observations, suggesting interactions involving multiple loci.

In this study we examined whether there are functional interaction between TLR3 and EP3. Moreover, we also examined whether there is an epistatic interaction between *TLR3* and *PTGER3* polymorphisms in patients with SJS/TEN with ocular surface complications.

This study was approved by the institutional review board of Kyoto Prefectural University of Medicine and the University of Tokyo, Graduate School of Medicine. All experimental procedures were conducted in accordance with the principles of the Helsinki Declaration. Details of the patients and methods are described in the Methods section in this article's Online Repository at www.jacionline.org. The primers and probes used in this study are shown in Table E1 in this article's Online Repository at www.jacionline.org.

First, we examined the functional interaction between TLR3 and EP3 by using *TLR3* KO, *PTGER3* KO, and *TLR3/PTGER3* double-knockout (DKO) mice in addition to our EAC model. We compared conjunctival eosinophil infiltration in wild-type, *TLR3* KO, *PTGER3* KO, and *TLR3/PTGER3* DKO mice. Although sensitization (intracutaneous and intraperitoneal injection of short ragweed pollen [RW; Polysciences, Inc, Warrington, Pa] adsorbed on aluminum hydroxide [200 µg of RW and 2.6 mg of alum]) without challenge (RW eye drop) did not affect the number of eosinophils after sensitization and challenge, the number of eosinophils in the lamina propria mucosae of the conjunctiva was significantly increased in all of them compared with those in PBS-challenged control animals, and the number after sensitization and challenge in *PTGER3* KO mice was significantly larger and significantly lower in *TLR3* KO than in wild-type mice, as

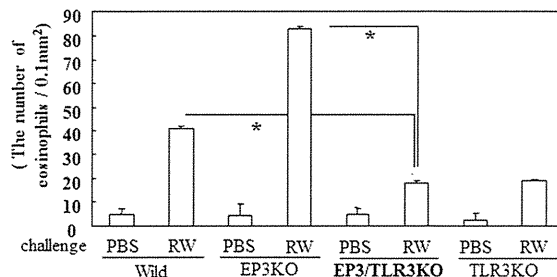


FIG 1. Functional interaction between EP3 and TLR3. In *TLR3/PTGER3* DKO mice the number of eosinophils in the lamina propria mucosae of the conjunctiva was decreased to a level similar to that seen in *TLR3* KO mice and was significantly lower than that seen in either *PTGER3* KO or wild-type mice. Data are shown as means ± SEMs of samples from all the mice examined (wild-type: phosphate-buffered saline, n = 24; RW, n = 28; *PTGER3* KO mice: phosphate-buffered saline, n = 23; RW, n = 25; EP3/TLR3 DKO mice: phosphate-buffered saline, n = 4; RW, n = 11; *TLR3* KO mice: phosphate-buffered saline, n = 12; RW, n = 12). **P* < .0005.

we have reported previously.^{1,2} Because TLR3 could regulate allergic inflammation in the absence of exogenous viral infection or the TLR3 ligand, it is possible that in our allergic conjunctivitis model endogenous RNA from tissues or cells stimulates TLR3.¹ With respect to EP3, one of the prostaglandin E receptors (EP1-EP4), our earlier observations suggested that during the elicitation phase of our EAC model, prostaglandin E₂ is synthesized in the conjunctival epithelium through microsomal prostaglandin E synthase 1.²

Furthermore, in *TLR3/PTGER3* DKO mice the number of eosinophils in the lamina propria mucosae of the conjunctiva was decreased to a level similar to the number of eosinophils in the lamina propria mucosae of the conjunctiva in *TLR3* KO mice and was significantly lower than the number of eosinophils in the lamina propria mucosae of the conjunctiva in not only *PTGER3* KO mice but also in wild-type mice (Fig 1). In addition, we previously reported that in human conjunctival epithelial cells the EP3 agonist suppressed the production of cytokines, such as thymic stromal lymphopoietin⁸ and RANTES,⁹ induced by polyinosinic:polycytidylic acid, a TLR3 ligand. Thymic stromal lymphopoietin and RANTES play important roles in the recruitment of eosinophils. These results suggest that EP3 negatively regulates the eosinophilic infiltration of EAC induced by TLR3, which causes reduced eosinophilic conjunctival inflammation in *TLR3/PTGER3* DKO mice, despite the pronounced eosinophilic conjunctival inflammation seen in *PTGER3* KO mice.

We have reported that the frequency of carriers of the HLA-A*0206 allele is significantly higher among Japanese patients with severe ocular surface complications.¹⁰ We have also performed SNP association analysis of candidate genes and documented the associated polymorphisms of several immune-related genes, including *TLR3*,³ IL-4 receptor (*IL4R*),¹¹ *IL13*, and Fas ligand (*FasL*) in Japanese patients with SJS/TEN. Furthermore, we have performed a genome-wide association study of the patients with SJS/TEN and found associations between 6 SNPs in the *PTGER3* gene and the Japanese patients with SJS/TEN.⁴

We carried out a statistical search for interactions between all possible pairs of loci by applying high-dimensional variable selection methods, such as Sure Independence Screening (SIS)

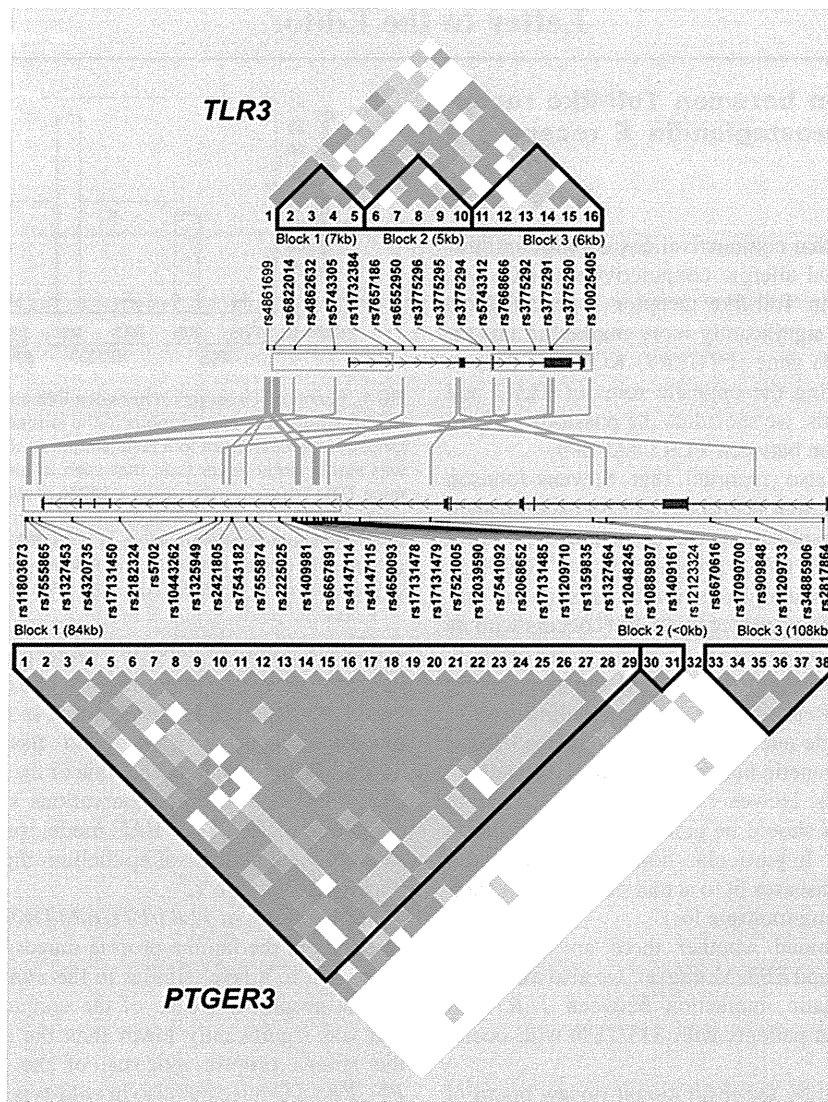


FIG 2. LD in EP3 and TLR3 regions. LD in the *TLR3* and *PTGER3* regions show 3 solid-spine LD blocks in each region. Iterative SIS reported 14 variables with nonzero regression coefficients, as if connecting the 5' region of *TLR3* and the 3' region of *PTGER3*.

and LASSO, to the comprehensive dataset obtained from our previous studies for a total of 14 immune-related genes (see Table E2 in this article's Online Repository at www.jacionline.org), including *PTGER3* and *TLR3*. After filtering with the standard SNP quality control filter, 36 SNPs were used for SIS to scan a total of 5778 ($3 \times 36 + 9 \times 36 \times [36-1]/2$) dummy variables. As a result, iterative SIS reported 2 variables with susceptible effects on SJS, which were involved in locus pairs of *PTGER3*-*TLR3* and *HLA-A-IL1A*, respectively (see Table E3 in this article's Online Repository at www.jacionline.org). The result showed that the *PTGER3* rs.4147114G/C SNP with the *TLR3* rs.3775296T/T SNP exhibited a higher odds ratio (OR, 25.3; $P = .000527$) than only the *PTGER3* rs.4147114G/C SNP (OR, 2.66; $P = .0023$) or only the *TLR3* rs.3775296T/T SNP (OR, 5.35; $P = .00025$). These 2 susceptible interactions were also confirmed by using LASSO.

Next, we focused on the epistatic interaction between *TLR3* and *PTGER3* and analyzed the additional 10 SNPs of *TLR3*

and 32 SNPs of *PTGER3*, resulting in a total of 17 SNPs of *TLR3* and 38 SNPs of *PTGER3*. All genotyping results agreed with Hardy-Weinberg equilibrium ($P > .01$) in both the case and control samples. These results showed that 5 additional SNPs of *TLR3* and 14 SNPs of *PTGER3*, a total of 7 SNPs of *TLR3* and 20 SNPs of *PTGER3*, were associated with SJS/TEN with ocular complications in addition to the previously reported 2 SNPs of *TLR3* and 6 SNPs of *PTGER3* (see Tables E4 and E5 in this article's Online Repository at www.jacionline.org). Moreover, we investigated disequilibrium (LD) in *TLR3* and *PTGER3* regions by using the squared correlation coefficient (1 SNP of *TLR3* [rs3775293] for which the minor allele frequency in both cases and control subjects was less than 5% was excluded) and identified 3 solid-spine LD blocks in each region. Iterative SIS reported 14 variables with nonzero regression coefficients as if connecting the 5' region of *TLR3* (block 1) and the 3' region of *PTGER3* (block 1, Fig 2).

We previously reported that the expression of EP3, the protein of the *PTGER3* gene, was downregulated in the conjunctival epithelium of patients with SJS/TEN with ocular surface complications.^{4,12}

Although *TLR3* mRNA expression might also be downregulated in patients with SJS/TEN (see Fig E2 in this article's Online Repository at www.jacionline.org), our immunohistologic analysis did not clearly detect downregulation of the protein (see Fig E3 in this article's Online Repository at www.jacionline.org).

In the conjunctival epithelium of patients with SJS/TEN, EP3 was remarkably downregulated, and TLR3 might also be downregulated. Because EP3 might be more strongly downregulated than TLR3 in these patients, it is possible that EP3 is incapable of preventing TLR3-associated inflammation in patients with SJS/TEN.

In conclusion, we have suggested the functional interaction between TLR3 and EP3 supported by their epistatic interaction that confers an increased risk for SJS with severe ocular surface complications.

Mayumi Ueta, MD, PhD^{a,b}
Gen Tamiya, PhD^c
Katsushi Tokunaga, PhD^d
Chie Sotozono, MD, PhD^e
Masao Ueki, PhD^c
Hiromi Sawai, PhD^d
Tutomu Inatomi, MD, PhD^e
Toshiyuki Matsuoka, MD, PhD^f
Shizuo Akira, MD, PhD^g
Shuh Narumiya, MD, PhD^h
Kei Tashiro, MD, PhD^g
Shigeru Kinoshita, MD, PhD^e

From the Departments of ^aOphthalmology and ^bGenomic Medical Sciences, Kyoto Prefectural University of Medicine, Kyoto, Japan; ^cthe Research Center for Inflammation and Regenerative Medicine, Faculty of Life and Medical Sciences, Doshisha University, Kyoto, Japan; ^dthe Advanced Molecular Epidemiology Research Institute, Faculty of Medicine, Yamagata University, Yamagata, Japan; ^ethe Department of Human Genetics, Graduate School of Medicine, University of Tokyo, Tokyo, Japan; ^fTenri Yorozu Hospital, Nara, Japan; ^gthe Department of Host Defense, Research Institute for Microbial Diseases, Osaka University, Osaka, Japan; and ^hthe Department of Pharmacology and Faculty of Medicine, Kyoto University, Kyoto, Japan. E-mail: mueta@koto.kpu-m.ac.jp.

Supported in part by grants-in-aid for scientific research from the Japanese Ministry of Health, Labour and Welfare, the Japanese Ministry of Education, Culture, Sports, Science and Technology; a research grant from the Kyoto Foundation for the Promotion of Medical Science; and the Intramural Research Fund of Kyoto Prefectural University of Medicine.

Disclosure of potential conflict of interest: S. Narumiya has received research support from One Pharmaceuticals Co Ltd. The rest of the authors declare they have no relevant conflicts of interest.

REFERENCES

1. Ueta M, Uematsu S, Akira S, Kinoshita S. Toll-like receptor 3 enhances late-phase reaction of experimental allergic conjunctivitis. *J Allergy Clin Immunol* 2009;123:1187-9.
2. Ueta M, Matsuoka T, Narumiya S, Kinoshita S. Prostaglandin E receptor subtype EP3 in conjunctival epithelium regulates late-phase reaction of experimental allergic conjunctivitis. *J Allergy Clin Immunol* 2009;123:466-71.
3. Ueta M, Sotozono C, Inatomi T, Kojima K, Tashiro K, Hamuro J, et al. Toll-like receptor 3 gene polymorphisms in Japanese patients with Stevens-Johnson syndrome. *Br J Ophthalmol* 2007;91:962-5.
4. Ueta M, Sotozono C, Nakano M, Taniguchi T, Yagi T, Tokuda Y, et al. Association between prostaglandin E receptor 3 polymorphisms and Stevens-Johnson syndrome identified by means of a genome-wide association study. *J Allergy Clin Immunol* 2010;126:1218-25, e10.
5. Stevens AM, Johnson FC. A new eruptive fever associated with stomatitis and ophthalmia: report of two cases in children. *Am J Dis Child* 1922;24:526-33.
6. Sotozono C, Ang LP, Koizumi N, Higashihara H, Ueta M, Inatomi T, et al. New grading system for the evaluation of chronic ocular manifestations in patients with Stevens-Johnson syndrome. *Ophthalmology* 2007;114:1294-302.
7. Cordell HJ. Detecting gene-gene interactions that underlie human diseases. *Nat Rev Genet* 2009;10:392-404.
8. Ueta M, Matsuoka T, Yokoi N, Kinoshita S. Prostaglandin E receptor subtype EP3 downregulates TSLP expression in human conjunctival epithelium. *Br J Ophthalmol* 2011;95:742-3.
9. Ueta M, Matsuoka T, Yokoi N, Kinoshita S. Prostaglandin E2 suppresses polyinosine-polycytidylic acid (polyI: C)-stimulated cytokine production via prostaglandin E2 receptor (EP) 2 and 3 in human conjunctival epithelial cells. *Br J Ophthalmol* 2011;95:859-63.
10. Ueta M, Sotozono C, Tokunaga K, Yabe T, Kinoshita S. Strong association between HLA-A*0206 and Stevens-Johnson syndrome in the Japanese. *Am J Ophthalmol* 2007;143:367-8.
11. Ueta M, Sotozono C, Inatomi T, Kojima K, Hamuro J, Kinoshita S. Association of IL4R polymorphisms with Stevens-Johnson syndrome. *J Allergy Clin Immunol* 2007;120:1457-9.
12. Ueta M, Sotozono C, Yokoi N, Inatomi T, Kinoshita S. Prostaglandin E receptor subtype EP3 expression in human conjunctival epithelium and its changes in various ocular surface disorders. *PLoS One* 2011;6:e25209.

doi:10.1016/j.jaci.2012.01.069

METHODS

Patients

This study was approved by the institutional review board of Kyoto Prefectural University of Medicine and the University of Tokyo, Graduate School of Medicine. All experimental procedures were conducted in accordance with the principles of the Helsinki Declaration. The purpose of the research and the experimental protocols were explained to all participants, and their prior written informed consent was obtained.

Diagnosis of SJS/TEN was based on a confirmed history of acute onset of high fever, serious mucocutaneous illness with skin eruptions, and involvement of at least 2 mucosal sites, including the ocular surface.

In the acute stage patients with SJS/TEN manifest vesiculobullous lesions of the skin (Fig E1, A) and mucosa (especially that of the eyes and mouth), severe conjunctivitis (Fig E1, B), and persistent corneal epithelial defects caused by ocular surface inflammation. Oral involvement, including blisters, erosions, and bleeding of the mouth and lips (Fig E1, C), has been observed in all patients with SJS/TEN with severe ocular surface complications, and almost all such patients lose their fingernails in the acute or subacute stage as a result of paronychia (Fig E1, D). In the chronic stage, despite healing of the skin lesions, ocular surface complications, including conjunctival invasion into the cornea (Fig E1, E), dry eyes, symblepharon, and in some instances keratinization of the ocular surface persist.

To investigate 44 SNPs of the 13 genes along with alleles of HLA-A analyzed by means of direct sequencing, we enrolled 61 patients with SJS/TEN in the chronic or subacute phase; all presented with symptoms of ocular surface complications. The control subjects were 130 healthy volunteers. All participants and volunteers were Japanese residing in Japan. The average age of the 61 patients and 160 control subjects was 45.3 ± 18.1 (SD) and 36.8 ± 11.9 (SD) years, respectively. The male/female ratios in the patient and control groups were 26/35 and 49/81, respectively.

Furthermore, we added 55 subjects and 91 control subjects to obtain a total of 116 case samples and 221 control samples for analysis of LD block around *TLR3* and *PTGER3*. The average age of the 116 patients and 221 control subjects was 44.0 ± 18.0 (SD) and 35.6 ± 11.1 (SD) years, respectively. The male/female ratios in the patient and control groups were 46/70 and 89/132, respectively.

SNP genotyping

For a search of the 44 SNPs of 13 genes along with HLA-A alleles (listed in Table E2), SNP genotyping was performed by using PCR direct sequencing. Genomic DNA was isolated from human peripheral blood at SRL, Inc (Tokyo, Japan). For direct sequencing, PCR amplification was conducted with AmpliTaq Gold DNA Polymerase (Applied Biosystems, Foster City, Calif) for 35 cycles at 94°C for 1 minute and annealing at 60°C for 1 minute and 72°C for 1 minute on a commercial PCR machine (GeneAmp; PerkinElmer, Applied Biosystems). The PCR products were reacted with BigDye Terminator version 3.1 (Applied Biosystems), and sequence reactions were resolved on an ABI PRISM 3100 Genetic Analyzer (Applied Biosystems).

To obtain more detailed information of genetic variants in the *TLR3* and *PTGER3* regions, we genotyped 116 patients with SJS/TEN and 221 healthy control subjects for 42 SNPs by using the DigiTag2 and TaqMan SNP genotyping assays (Applied Biosystems). In the DigiTag2 assay we designed multiplex PCR primers for each of the 32 SNP sites. Multiplex PCR was performed in 10 μ L of Multiplex PCR buffer containing 25 ng of genomic DNA, 25 nmol/L of each multiplex primer mix, 200 μ mol/L of each deoxyribonucleoside triphosphate, 2.25 mmol/L $MgCl_2$, and 0.4 U of KAPA2G Fast HotStart DNA polymerase (Kapa Biosystems, Woburn, South Africa). Cycling was performed at 95°C for 3 minutes, followed by 40 cycles of 95°C for 15 seconds and 68°C for 2 minutes. We used 36 SNPs covering a greater than 95% call rate for further analyses (Table E1). In the TaqMan SNP genotyping assay PCR amplification was performed in a 5- μ L reaction mixture containing 1 μ L of genomic DNA, 2.5 μ L of Absolute QPCR ROX Mix (Thermo Fisher Scientific, Inc, Waltham, Mass), and $\times 40$ TaqMan SNP Genotyping Assay probe (Applied Biosystems) for each SNP. The QPCR thermal cycling program was 95°C for 15 minutes, followed by 40 cycles of 95°C for

15 seconds and 60°C for 1 minute. All samples subjected to the DigiTag2 assay and the TaqMan SNP genotyping assay were found to have a greater than 95% call rate. The 7 SNPs of *TLR3* and 6 SNPs of *PTGER3*, which we have reported previously, were examined by using PCR direct sequencing, as described above. The primers and probes used in this study are shown in Table E3.

HLA-A genotyping

For HLA-A genotyping, we performed PCR amplification followed by hybridization with sequence-specific oligonucleotide probes (PCR-SSO) by using commercial bead-based typing kits (WAK Flow; Wakunaga, Hiroshima, Japan).

Statistical analysis

A scan for epistatic interactions in data for multiple loci is associated with serious problems, such as computational burden and high dimensionality. The former restricts potential algorithms to those that are simple and fast, whereas the latter is a theoretic issue with no efficient and universal solution, being known as the “ $p > n$ or $p \gg n$ problem” or the “curse of dimensionality,” causing standard methods of multivariate regression to break down and prohibitive conservation of alternate methods involving multiple univariate regression caused by necessary corrections of the heavy multiplicity. On the other hand, eclectic methods based on SNP filtering by P value could potentially miss interactions with no or only weak marginal effects. Instead of these current methods, we have therefore proposed the use of a model selection strategy for interaction analysis of high-dimensional data. Our new software, EPISIS, implements SIS (Fan and Lv 2008), followed by some iterative steps, which can be roughly regarded as a sophisticated analog of the classical forward-backward stepwise procedure suited to ultra-high-dimensional regression models. SIS has 2 major parts: screening and variable selection. In the screening part candidates are selected on the basis of feature ranking, and then subsequent variable selection from these candidates is carried out for interactions and main effects. As a variable selection algorithm for penalized regression, we use SCAD. We also use LASSO for comparison.

Statistical significance of the association with each SNP was assessed by using the Fisher exact test on 2×2 contingency tables. Haploview software (version 4.2) was used to infer the LD structure of specific genomic regions, to perform haplotype association testing, and to permute the data pertaining to their association.

Mice

BALB/c mice were purchased from CLEA (Tokyo, Japan) and used at 6 to 12 weeks of age for sensitization. *TLR3* KO and *PTGER3* KO mice were generated, as described previously, and back-crossed for more than 7 generations to BALB/c mice. *TLR3/PTGER3* DKO mice were generated by interbreeding of *TLR3* KO and *PTGER3* KO mice at Kyoto Prefectural University of Medicine. They were subjected to EAC at 9 to 15 weeks of age, with age-matched, wild-type BALB/c mice as control animals. The mice were maintained on a 12-hour/12-hour light/dark cycle under specific pathogen-free conditions. All experimental procedures were approved by the Committee on Animal Research of Kyoto Prefectural University of Medicine, Kyoto, Japan. All studies were performed in accordance with the Association for Research in Vision and Ophthalmology’s “Statement for the use of animals in ophthalmic and vision research.”

Eosinophil infiltration in a murine model of EAC

The experiments were conducted by using a protocol approved by the Institutional Animal Care and Use Committee of Kyoto Prefectural University of Medicine. Short RW was purchased from Polysciences, Inc (Warrington, Pa), and aluminum hydroxide (alum) was from Sigma-Aldrich (St Louis, Mo). The mice were immunized with an intracutaneous injection of RW adsorbed on alum (200 μ g of RW and 2.6 mg of alum) into the left hind footpad on day 0. On day 7, they received an intraperitoneal injection of RW adsorbed on alum, and on day 18, their eyes were challenged with RW in PBS (500 μ g in 5 μ L per

eye) or with PBS alone (5 μ L per eye). Their eyes, including the conjunctiva, were harvested 24 hours after the last challenge, fixed in 10% neutral-buffered formalin, and embedded in paraffin blocks for histologic analysis. Vertical 6- μ m-thick sections were mounted on microscope slides, deparaffinized, and stained with Luna stain, which identifies erythrocytes and eosinophil granules.

Using an entire section from the central portion of the eye, including the pupil and optic nerve head, we counted infiltrating eosinophils in the lamina propria mucosae of the tarsal conjunctiva. Cell counts were expressed as the number of infiltrating eosinophils per unit area (0.1 mm²) measured with image software (Scion Corp, Frederick, Md).

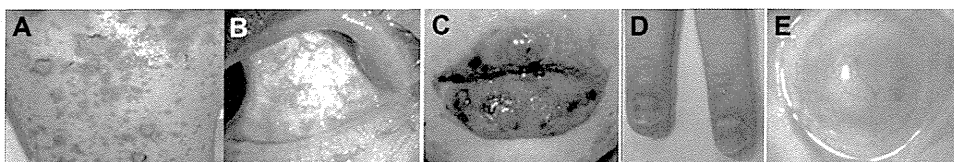


FIG E1. Features of patients with SJS/TEN with ocular complications. **A**, Vesiculobullous lesions of the skin in the acute stage. **B**, Severe conjunctivitis in the acute stage. **C**, Oral involvement, including blisters, erosions, and bleeding of the mouth and lips in the acute stage. **D**, Paronychia in the acute stage. **E**, Conjunctival invasion into the cornea in the chronic stage.

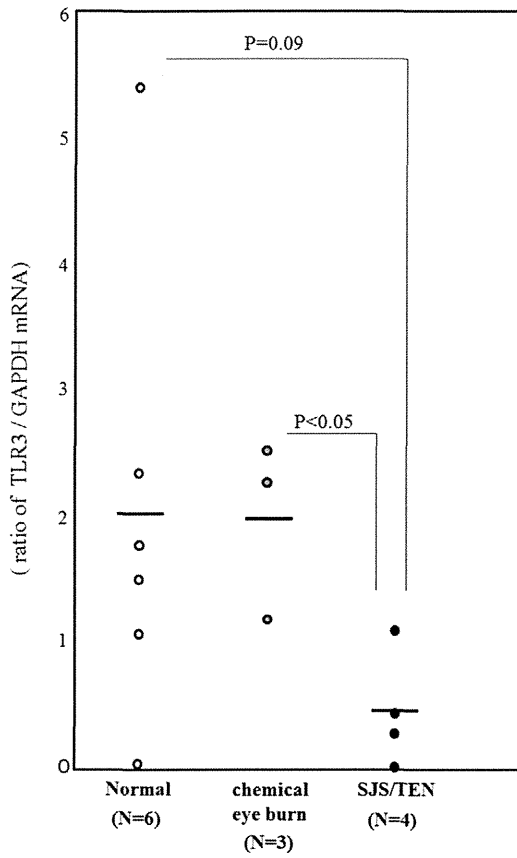


FIG E2. Expression of *TLR3* mRNA in conjunctival tissues from patients with SJS/TEN and chemical eye burn and the control subjects. Total RNA was isolated from conjunctival tissue sections by using the RNeasy mini kit (Qiagen, Hilden, Germany), according to the manufacturer's instructions. The RT reaction was with the SuperScript preamplification kit (Invitrogen, Carlsbad, Calif). Quantitative RT-PCR was on an ABI-prism 7700 instrument (Applied Biosystems). The probes for human *TLR3* and human glyceraldehyde-3-phosphate dehydrogenase (*GAPDH*) were from Applied Biosystems. The results were analyzed with sequence detection software (Applied Biosystems). The quantification data were normalized to the expression of the housekeeping gene *GAPDH*.

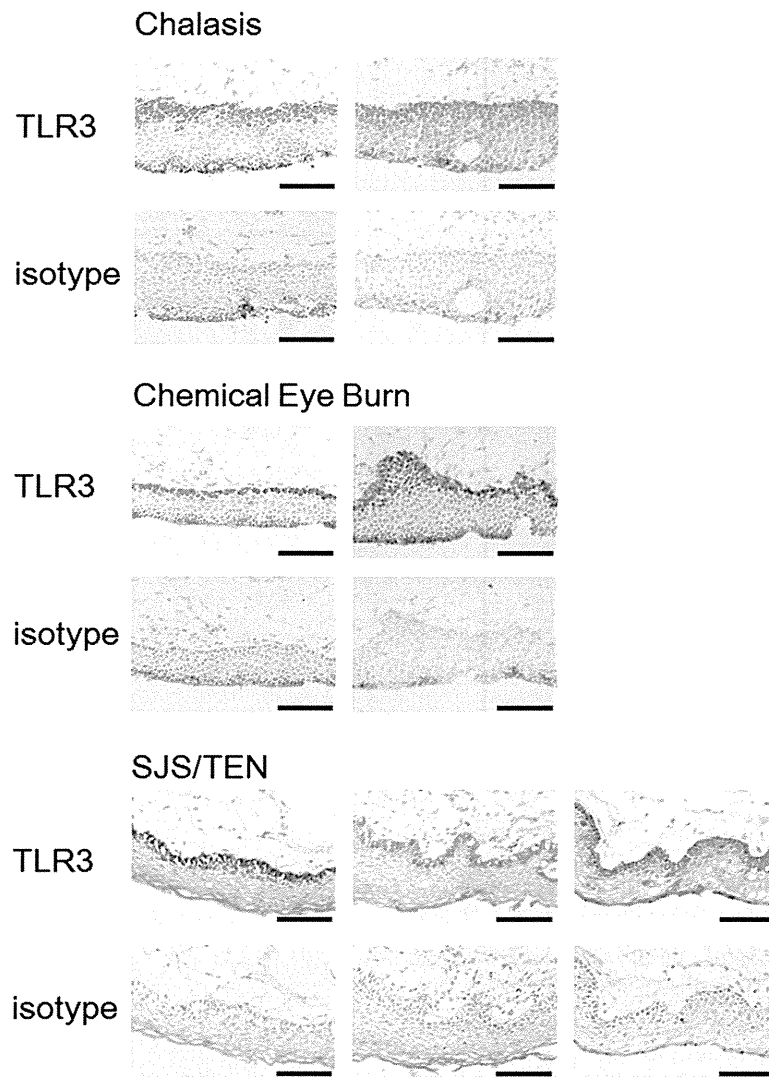


FIG E3. Immunohistologic analysis of *TLR3* in conjunctival epithelium of patients with SJS/TEN and chemical eye burn and control subjects. For TLR3 staining, we used rabbit polyclonal antibody to TLR3 (Abcam, Cambridge, Mass). The secondary antibody (Biotin-SP-conjugated AffiniPure F[ab']₂ fragment donkey anti-rabbit IgG [H+L], 1:500 dilution; Jackson ImmunoResearch, Baltimore, Md) was applied for 30 minutes. The VECTASTAIN ABC reagent (Vector Laboratories, Burlingame, Calif) was used for increased sensitivity with peroxidase substrate solution (DAB substrate kit; Vector Laboratories) as a chromogenic substrate. Each scale bar represents 100 μ m.

TABLE E1. Primers and probes used in SNP analysis of *TLR3* and *PTGER3*

Gene	rsID	Genotyping	Primer sequence or context sequence (VIC/FAM)
<i>TLR3</i>	rs4861699	DigiTag2	AACCTAAAGAAGTGAAAGACTTGAACACTGAAAACATAA AGGTATTTAAACTAATTTGAGTGGATTTTTGTGTATGGTGTA
	rs6822014	DigiTag2	ATAACTTGATGAGCTTGAAGACAAGTATACTTCTGTGAAA GGCATAACATACAATGGAATATTATTCTACCTTACAAAA
	rs4862632	DigiTag2	GCTTGATCTGCAAACATAAGTGACATACGCAAACATAATA ACCATTTGTTTAGGTTTATAATATATTTCATCGCATTACATA
	rs5743305	DigiTag2	ACTCACTTTTTTTCATTACAGATGTGCTATGATCTATTATA CAAGGCGCTCACAGAGAAGAAATCTTTGAATATTAGTGAA
	rs11732384	DigiTag2	AAATTATTCCAGGTAAGTGTCAAGGTAATAAAATCACCTTA GAGGGGTACATCTCACCTAAGCAAGGAGAATGTATTGTA
	rs7657186	DigiTag2	AGGCCAATACCACATTGTTTCGGATTACTTTAGCTTTACAA CAACCACCACACACTTTTAAACGACCGAATCTCATAA
	rs6552950	DigiTag2	TGTTGCACCACCACTTTCTGACAACATTTGGTA ATTAACCTTAGGAGAGGTCACACACCTTCACATAGAAGCTAA
	rs5743312	DigiTag2	TCCTATGAAGCAGAGTCAATTATCACGCCATTTGAAA AGTTGTCATCGAATCAAATTAAGAGGTAAGAAGTAAGGTA
	rs7668666	DigiTag2	AGTGCCTTAACAGTGTGAATTTTCAGTACAGTAAGAATTTAA GAGGGCTACGTGTCCTGGATCATGAAGACAGACTA
	rs3775292	DigiTag2	GAGAAAATCCGGGTGGAAAGACGAGAGGGAGAGCTA GACAGATTCCGAATGCTTGTGTTGCTAATCCAAACATA
	rs3775291	DigiTag2	AAGCAATATGTTACAGGATTGATAAACCTGAAATACCTA TTGGCTATGTTGTTGTTGCTTAGATCCAGAATGGTCAA
	rs10025405	DigiTag2	AGCTATTCAAGTCTATTTCCTAATAATCAGATTCTCTTTATTGTA GTTTCAATGGGTATAATGCTATTTCCTTTGTAAAAGAGTA
	rs3775296	Direct sequencing	TTACCTTCTGCTTGACAAAGGG TGCATTGAAAGCCATCTGC
	rs3775295	Direct sequencing	TCACATGGCTTATCAAACACACAG
	rs3775294	Direct sequencing	CATTGCTCTTCTCAGATGCC
	rs3775293		CAGTTCTTTACTCCATCTCCGC
	rs3775292	Direct sequencing	CCAAGGCTCTGGTAAGGGTG
	rs3775291		TGGCTAAAATGTTTGGAGCA
	rs3775290	Direct sequencing	GAAGAGGCTGGAATGGTGAA
<i>PTGER3</i>	rs11803673	DigiTag2	GAAACACATCCTGGAGTCATTCTGATGGGATTGCTA GGACAGGGAGAGAGGGACGGAAAGAAAAATAATCAA
	rs7555865	DigiTag2	GAAACACATCCTGGAGTCATTCTGATGGGATTGCTA GGACAGGGAGAGAGGGACGGAAAGAAAAATAATCAA
	rs1327453	DigiTag2	AGTTACCATAACACAAATGGAAAACACACATAACATGATGA TCAGTCAACCTAACTGGTCTTCTACCCAGTCAATTCATAA
	rs4320735	DigiTag2	AGACTTGAGTCTAGAATTGCTTTGTTGAGAGAGATAGGTA TGCAAGTGACAGAAATCAAAGTCAATTTAGCTTAGGTATA
	rs2182324	DigiTag2	ATAATGCCATCTTGCTACTATGTAGAGCAGAAACTTTCAA CCATAAGGGTTTAAAATCTTTATTCACTTCACTGATGTATA
	rs10443262	DigiTag2	GACAGCCATCACAGGATCAAAGACCTAGGAAGGAA TAGTCTCATTGACTCCATGCCCATATGCTGGACA
	rs2421805	DigiTag2	AGATACGTAATGAAAGTGGTCTCTTGTTTGGTCTCTCTTA ACACAGAGAGGCCTAACACTGAAAACCAATGACATAAAAA
	rs2225025	DigiTag2	GGAAGGTCACCTACAAAGGGAACCCTATCAAGCTAA TTTCTTTCCATATTAGCACTCCCTTAATGACTGTGCAA
	rs1409981	DigiTag2	TAGGGGATGTGAGAAGGAGGGTCTGAAGATGAAA AAGCTGCCTTTACCCATACCTATTTGAGTTACTCAGAAA
	rs6667891	DigiTag2	TAGGGGATGTGAGAAGGAGGGTCTGAAGATGAAA AAGCTGCCTTTACCCATACCTATTTGAGTTACTCAGAAA
	rs4147115	DigiTag2	CCTGAAACTCCATATTTTACAACCTCACCTCTGTGATTTTCA ATCCTAACCAAGTTACTTTGTCTTATCAGTTTTAGCACTTA
	rs4650093	DigiTag2	CCTGAAACTCCATATTTTACAACCTCACCTCTGTGATTTTCA ATCCTAACCAAGTTACTTTGTCTTATCAGTTTTAGCACTTA
	rs17131478	DigiTag2	CCTGAAACTCCATATTTTACAACCTCACCTCTGTGATTTTCA ATCCTAACCAAGTTACTTTGTCTTATCAGTTTTAGCACTTA
	rs17131479	DigiTag2	CCTGAAACTCCATATTTTACAACCTCACCTCTGTGATTTTCA ATCCTAACCAAGTTACTTTGTCTTATCAGTTTTAGCACTTA
	rs7521005	DigiTag2	ATGAACACTGACATATGAACCTAAAAGCTAGAAATTTAACTAAA CTTTTCTCAGATCCTCATCTCCTCATGCAATATGCCATAA

(Continued)

TABLE E1. (Continued)

Gene	rsID	Genotyping	Primer sequence or context sequence (VIC/FAM)
	rs12039590	DigiTag2	AGAGTGTGGACTATCACTTGTGCAAATATTTGAGAAAATA AGGTATGTGAATCCTTATAACAGTCTTAAGGAGTAGACGTTA
	rs7541092	DigiTag2	AGGGAGATACAAATCAAACAAAAACATGTTGAAGTCAATA CATCTACAGGTCAAGAAATGCCTAGGAATGCCAGAAAA
	rs2068652	DigiTag2	AGGGAGATACAAATCAAACAAAAACATGTTGAAGTCAATA CATCTACAGGTCAAGAAATGCCTAGGAATGCCAGAAAA
	rs17131485	DigiTag2	CTGTGGAGAAGAATCTACCACCTTGATCTGGAGTTGTA GTTTGATTTGTATCTCCCTAAAATATCATCAGTTCTTCAA
	rs11209710	DigiTag2	AGTATTGAAGAGTCTAATACTGAGTCATTGAAGGATATAGTA ATGCTTGAAGAATGCTCCAAGAAATGGACTATTCTCATATA
	rs1359835	DigiTag2	AGTATTGAAGAGTCTAATACTGAGTCATTGAAGGATATAGTA ATGCTTGAAGAATGCTCCAAGAAATGGACTATTCTCATATA
	rs1327464	DigiTag2	CTGCTTTGTAACCTGGGCTTGGAGAGGTTTATCCAA CTTCAATACTTCACTAGACTTTCTGGATGCAATGACTGTA
	rs12048245	TaqMan	TCTAGGAGATTCTGAGACAGGTGTT[C/T]GCTTCAAAGGAAAAGCTTTGAAA
	rs10889897	TaqMan	AGGAAAGGCATCAAAGGAATTGCAC[A/G]GGGTAGGAAAGTACAACGGATATTC
	rs1409161	TaqMan	CTTAATTTTAGGCTTCTGGTCTCCA[A/G]AACTGGAAGAAAAATGTTTGGGTA
	rs12123324	TaqMan	GAAGCTCCTCAAGTGTAGAGTTCA[C/T]AAGATGTTGGGTAACGTACAGTTT
	rs6670616	TaqMan	TAAAGACGAATAAATACAGCTGTGT[A/T]TTGATTCCGCACCTTTTCCTATGACA
	rs17090700	TaqMan	CATGACATTTGGGATTAAGTTCTGC[A/C]TTTGTAGTACTCATTATTGAAGT
	rs909848	TaqMan	TCATTAATAGTTCTTTCTGCTCACC[C/T]ACACTAGCTCACTAATTTATCCCCA
	rs11209733	TaqMan	ATTTGTAAGTATATTAGCATTAA[C/G]TGTAGTCATCCTACAGGAGTATAGA
	rs17131450	Direct sequencing	TTTTATGCAGCTTTCGGTCA CCCCTCCAGGCTGATAACTC
	rs5702	Direct sequencing	CAAGTAGCAGTTGGCAGCAA TGCAATCAGACAGGCAAGAG
	rs1325949	Direct sequencing	AATTGCAAGTCCAGCTCAGG AGGCCTCAGGGAGCTTTTAC
	rs7543182	Direct sequencing	TGTGAGGCAAGAACCAGACA AGGACCTGGGAGGGAAGATA
	rs7555874	Direct sequencing	AAGCCAGCAAAGGACAAGAA TGTGTGTGTCTGCCAGGTT
	rs4147114	Direct sequencing	TGCTGGAAGCTCATGGTCTA TGCATGGTTCGTCTAACCTTAT

TABLE E2. List of SNPs carried out in a statistical search for interactions

Symbol	Name	Chr	RefSeq allele	Note
PTGER3	Prostaglandin E receptor EP3	chr1		
	rs17131450		A/G	Genomic
	rs5702		C/T	Synonymous
	rs1325949		A/G	Intronic
	rs7543182		A/C	Intronic
	rs7555874		C/T	Intronic
	rs4147114		C/G	Intronic
IL13	Interleukin 13	chr5		
	rs1800925		C/T	Genomic
	rs20541		C/T	Missense
	rs1295685		C/T	3'UTR
TLR3	Toll-like receptor 3	chr4		
	rs3775296		G/T	Intronic
	rs3775295		C/T	Intronic
	rs3775294		C/T	Intronic
	rs3775293		C/T	Intronic
	rs3775292		C/G	Intronic
	rs3775291		A/G	Missense
FasL	Fas ligand	chr1		
	rs3830150		A/G	Intron of C1orf9
	rs2859247		C/T	Genomic
	rs2639614		A/G	Genomic
IL4R	Interleukin 4 receptor	chr16		
	rs1805010		A/C/G/T	Missense
	rs1805015		C/T	Missense
	rs1801275		A/G	Missense
MAIL	Nuclear factor of kappa light polypeptide gene enhancer in B-cells inhibitor, zeta	chr3		
	rs3821727		C/G	Missense
	rs677011		A/G	Intronic
	rs595788		C/T	Intronic
	rs3217713		indel	Intronic
	rs14134		A/G	Synonymous
	rs622122		A/T	Intronic
rs2305991	A/G	3'UTR		
IL4	Interleukin 4	chr5		
IL1A	Interleukin 1, alpha	chr2		
	rs2243250		C/T	
	rs2071376		A/C	Intronic
	rs2071375		A/G	Intronic
	rs2071373		C/T	Intronic
TLR2	Toll-like receptor 2	chr4		
	rs1894399		A/G	Intronic
	rs1609682		A/C	Intronic
	rs3804100			Synonymous
TLR5	Toll-like receptor 5	chr1		
	rs3804099			Synonymous
	rs2072493		A/G	Missense
PTGER4	Prostaglandin E receptor 4	chr5		
	rs5744168		A/C/G/T	STOP
Chr5p13	Genes in cytogenetic band chr5p13	chr5		
	rs1494558		A/C/G/T	Missense
GNLY	Granulysin	chr2		
	rs6871834		A/G	Genomic
	rs3755007		A/C	Genomic

TABLE E3. Susceptible interactions between loci detected by using Interactive Sure Independence Screening

Locus 1	Locus 2	OR	95% CI	P value
<i>PTGER3</i> rs4147114 (GC)	<i>TLR3</i> rs3775296 (TT)	25.3	3.2-203	.0000527
<i>PTGER3</i> rs4147114 (GC)	—	2.66	1.4-5.0	.0023
—	<i>TLR3</i> rs3775296 (TT)	5.35	2.0-14.1	.00025
<i>HLA-A*02:06</i>	<i>IL1A</i> rs1609682 (CA)	9.66	2.0-47.0	.00193
<i>HLA-A*02:06</i>	—	3.46	1.8-6.8	.0002
—	<i>IL1A</i> rs1609682 (CA)	—	—	.31

Boldface text indicates the pairs with interactions.

TABLE E4. Association between *TLR3* SNPs and SJS/TEN with ocular complications

rs no. of SNP	Frequencies of genotypes (%)			Allele 1 vs allele 2	Genotype 11 vs 12+22	Genotype 11+12 vs 22
	Genotypes	Controls	Cases	P value* OR (95% CI)	P value* OR (95% CI)	P value* OR (95% CI)
rs4861699	11 G/G	39.8	58.6	.0018	.001	.17
	12 G/A	47.5	33.6	1.76 (1.2-2.5)	2.14 (1.4-3.4)	—
	22 A/A	12.7	7.8	—	—	—
rs6822014	11 A/A	61.9	50.5	.00071	.048	.00008
	12 A/G	33.9	32.4	0.54 (0.4-0.8)	0.63 (0.4-1.0)	0.21 (0.1-0.5)
	22 G/G	4.2	17.1	—	—	—
rs11732384	11 G/G	51.6	65.5	.032	.014	.68
	12 G/A	41.2	28.4	1.52 (1.0-2.2)	1.78 (1.1-2.8)	—
	22 A/A	7.2	6.0	—	—	—
rs3775296†	11 G/G	51.6	44.0	.0046	.18	.00009
	12 G/T	43.0	37.1	0.61 (0.4-0.9)	—	0.25 (0.1-0.5)
	22 T/T	5.4	19.0	—	—	—
rs5743312	11 C/C	54.1	46.6	.0059	.19	.0001
	12 C/T	41.4	36.2	0.62 (0.4-0.9)	—	0.23 (0.1-0.5)
	22 T/T	4.6	17.2	—	—	—
rs7668666	11 C/C	39.4	30.4	.01	.11	.0069
	12 C/A	47.9	45.2	0.65 (0.5-0.9)	—	0.45 (0.3-0.8)
	22 A/A	12.7	24.3	—	—	—
rs3775290†	11 G/G	38.5	34.5	.057	.47	.0069
	12 G/A	50.2	43.1	—	—	0.44 (0.2-0.8)
	22 A/A	11.3	22.4	—	—	—

*P value for allele or genotype frequency comparison between cases and controls by using the χ^2 test.

†Italic rs numbers show previously reported SJS/TEN-associated SNPs.

TABLE E5. Association between *PTGER3* SNPs and SJS/TEN with ocular complications

rs no. of SNP	Frequencies of genotypes (%)			Allele 1 vs allele 2	Genotype 11 vs 12+22	Genotype 11+12 vs 22
	Genotypes	Controls	Cases	P value* OR (95% CI)	P value* OR (95% CI)	P value* OR (95% CI)
rs7555865	11 C/C	47.9	45.7	.10	.69	
	12 C/T	42.5	34.5	—	—	0.43 (0.2-0.8)
	22 T/T	9.6	19.8	—	—	
rs17131450†	11 C/C	87.8	76.7	.00069	.0086	.0039
	12 C/T	11.8	18.1	0.41 (0.2-0.7)	0.46 (0.3-0.8)	0.08 (0.01-0.7)
	22 T/T	0.5	5.2	—	—	—
rs5702†	11 C/C	49.3	64.7	.059	.0072	.6
	12 C/T	43.0	25.9	—	1.88 (1.2-3.0)	—
	22 T/T	7.7	9.5	—	—	—
rs1325949†	11 A/A	47.5	69.0	.0035	.00017	.88
	12 A/G	44.3	22.4	1.8 (1.2-2.6)	2.5 (1.5-3.9)	—
	22 G/G	8.1	8.6	—	—	—
rs2421805	11 T/T	48.1	33.6	.0014	.012	.0045
	12 T/G	44.4	48.7	0.58 (0.4-0.8)	0.55 (0.3-0.9)	0.37 (0.2-0.8)
	22 G/G	7.4	17.7	—	—	—
rs7543182†	11 G/G	50.7	70.7	.0096	.00041	.54
	12 G/T	42.5	20.7	1.67 (1.1-2.5)	2.34 (1.5-3.8)	—
	22 T/T	6.8	8.6	—	—	—
rs.7555874†	11 G/G	50.7	69.8	.014	.00074	.54
	12 G/A	42.5	21.6	1.62 (1.1-2.4)	2.25 (1.4-3.6)	—
	22 A/A	6.8	8.6	—	—	—
rs1409981	11 G/G	84.7	73.3	.0021	.012	.040
	12 G/A	13.0	19.8	0.48 (0.3-0.8)	0.49 (0.3-0.9)	0.32 (0.1-1.0)
	22 A/A	2.3	6.9	—	—	—
rs.4147114†	11 C/C	24.4	43.1	.0012	.00042	.10
	12 C/G	53.4	42.2	1.72 (1.2-2.4)	2.34 (1.5-3.8)	—
	22 G/G	22.2	14.7	—	—	—
rs4147115	11 A/A	25.5	39.5	.023	.0098	.34
	12 A/T	46.7	37.6	1.46 (1.1-2.0)	1.91 (1.2-3.1)	—
	22 T/T	27.8	22.9	—	—	—
rs4650093	11 C/C	51.4	65.5	.092	.013	.44
	12 C/T	42.3	25.9	—	1.8 (1.1-2.9)	—
	22 T/T	6.4	8.6	—	—	—
rs17131478	11 G/G	61.6	74.6	.035	.018	.79
	12 G/T	34.2	21.9	1.59 (1.0-2.5)	1.8 (1.1-3.0)	—
	22 T/T	4.1	3.5	—	—	—
rs17131479	11 C/C	62.2	75.0	.039	.018	.91
	12 C/G	34.1	21.6	1.58 (1.0-2.4)	1.8 (1.1-3.0)	—
	22 G/G	3.7	3.4	—	—	—
rs7521005	11 A/A	51.6	65.5	.10	.014	.44
	12 A/G	42.1	25.9	—	1.8 (1.1-2.8)	—
	22 G/G	6.3	8.6	—	—	—
rs7541092	11 G/G	62.4	74.8	.040	.023	.77
	12 G/A	33.5	21.7	1.57 (1.0-2.4)	1.8 (1.1-3.0)	—
	22 A/A	4.1	3.5	—	—	—
rs1359835	11 G/G	88.6	79.1	.0047	.019	.030
	12 G/C	10.9	17.4	0.45 (0.3-0.8)	0.49 (0.3-0.9)	0.13 (0.01-1.1)
	22 C/C	0.5	3.5	—	—	—
rs1327464	11 G/G	88.2	78.4	.0043	.017	.031
	12 G/A	11.3	18.1	0.46 (0.3-0.8)	0.49 (0.3-0.9)	0.13 (0.01-1.1)
	22 A/A	0.5	3.4	—	—	—
rs1409161	11 G/G	30.8	25.9	.040	.35	.014
	12 G/A	51.6	44.8	0.72 (0.5-1.0)	—	0.52 (0.3-0.9)
	22 A/A	17.6	29.3	—	—	—
rs34885906	11 T/T	85.5	94.0	.026	.021	.0
	12 T/C	14.5	6.0	2.5 (1.1-5.8)	2.6 (1.1-6.2)	—
	22 C/C	0.0	0.0	—	—	—
rs2817864	11 T/T	53.4	61.2	.056	.17	.021
	12 T/G	40.3	37.9	—	—	7.8 (1.0-59.9)
	22 G/G	6.3	0.9	—	—	—

*P value for allele or genotype frequency comparison between cases and controls by using the χ^2 test.

†Italic rs numbers show previously reported SJS/TEN-associated SNPs.

RESEARCH LETTERS

Downregulation of Monocyte Chemoattractant Protein 1 Expression by Prostaglandin E₂ in Human Ocular Surface Epithelium

Elsewhere, we reported that in the tears and serum of patients with acute-stage Stevens-Johnson syndrome or toxic epidermal necrolysis, the levels of interleukin 6 (IL-6), IL-8, and monocyte chemoattractant protein 1 (MCP-1) were dramatically increased.¹ We also reported that Stevens-Johnson syndrome or toxic epidermal necrolysis with severe ocular complications was associated with polymorphism of the prostaglandin E receptor 3 (EP₃) gene (*PTGER3*).²

Prostanoids are a group of lipid mediators that form in response to various stimuli. They include prostaglandin D₂ (PGD₂), PGE₂, PGF_{2α}, PGI₂, and thromboxane A₂. There are 4 subtypes of the PGE receptor: EP₁, EP₂, EP₃, and EP₄. We previously reported that PGE₂ suppresses polyinosine–polycytidylic acid (polyI:C)–stimulated cytokine production via EP₂ and/or EP₃ in human ocular surface epithelial cells.^{3,4} PolyI:C is a ligand of Toll-like receptor 3, which is strongly expressed in ocular surface epithelium.⁵ We found that PGE₂ suppresses the production of IL-6, chemokine (C-X-C motif) ligand 10, chemokine (C-X-C motif) ligand 11, and chemokine (C-C motif) ligand 5 but not IL-8 by epithelial cells on the human ocular surface³; it remains to be determined whether it also suppresses MCP-1 production. Monocyte chemoattractant protein 1 plays a significant role in the recruitment of monocytes and lymphocytes to the site of cellular immune reactions. In this study, we investigated whether PGE₂ downregulates polyI:C-induced MCP-1 production.

All experiments were conducted in accordance with the principles set forth in the Declaration of Helsinki. Enzyme-linked immunosorbent assay and quantitative real-time polymerase chain reaction were performed with primary human conjunctival epithelial cells and immortalized human corneal limbal epithelial cells using previously described methods (eAppendix, <http://www.archophthalmol.com>).³

First, we examined whether PGE₂ downregulated the production and messenger RNA (mRNA) expression of MCP-1 induced by polyI:C stimulation in human conjunctival and corneal epithelial cells. We found that it significantly attenuated the production of MCP-1 (Figure, A). Quantitative real-time polymerase chain reaction confirmed that the mRNA expression of MCP-1 was significantly downregulated by PGE₂ (Figure, A).

Next, we examined which PGE₂ receptor(s) contributed to the downregulation of polyI:C-induced MCP-1. We used the EP₂ agonist ONO-AE-259, the EP₃ agonist ONO-AE-248, and the EP₄ agonist ONO-AE-329. Enzyme-linked immunosorbent assay showed that the EP₂ and EP₃ agonists significantly suppressed the polyI:C-induced production of MCP-1, while the EP₄ agonist did not exert suppression (Figure, B). Quantitative real-time polymerase chain reaction confirmed that the EP₂ and EP₃ agonists significantly downregulated the mRNA expression of MCP-1 (Figure, C). Thus, our results document that PGE₂ attenuated the mRNA expression and production of MCP-1 via both EP₂ and EP₃.

In human macrophages, PGE₂ attenuated the lipopolysaccharide-induced mRNA and protein expression of chemokines including MCP-1 through EP₄.⁶ On the other hand, we demonstrated that in human ocular surface epithelial cells, PGE₂ attenuated the polyI:C-induced mRNA and protein expression of MCP-1 through EP₂ and EP₃ but not EP₄. Our findings suggest that EP₂ and EP₃ play important roles in the regulation of inflammation in epithelial cells, while EP₂ and EP₄ have important roles in immune cells such as macrophages.

In the tears and serum of patients with acute-stage Stevens-Johnson syndrome or toxic epidermal necrolysis, the levels of IL-6, IL-8, and MCP-1 were dramatically increased.¹ Although IL-8 was not regulated by PGE₂, IL-6 was regulated by PGE₂ via EP₃ in human ocular surface epithelial cells.³ Herein, we demonstrated that MCP-1 could be regulated by PGE₂ via EP₂ and EP₃. The regulation of cytokine production by PGE₂ may be associated with the pathogenesis of Stevens-Johnson syndrome or toxic epidermal necrolysis with severe ocular complications because it was associated with polymorphism of the EP₃ gene (*PTGER3*), one of the PGE receptors (EP₁, EP₂, EP₃, EP₄).²

In summary, our results show that MCP-1 produced by human ocular surface epithelial cells could be downregulated by PGE₂ via EP₂ and EP₃.

Mayumi Ueta, MD, PhD
Chie Sotozono, MD, PhD
Norihiko Yokoi, MD, PhD
Shigeru Kinoshita, MD, PhD

Author Affiliations: Research Center for Inflammation and Regenerative Medicine, Faculty of Life and Medical Sciences, Doshisha University (Dr Ueta) and Department of Ophthalmology, Kyoto Prefectural University of Medicine (Drs Ueta, Sotozono, Yokoi, and Kinoshita), Kyoto, Japan.

Correspondence: Dr Ueta, Department of Ophthalmology, Kyoto Prefectural University of Medicine, 465 Ka-

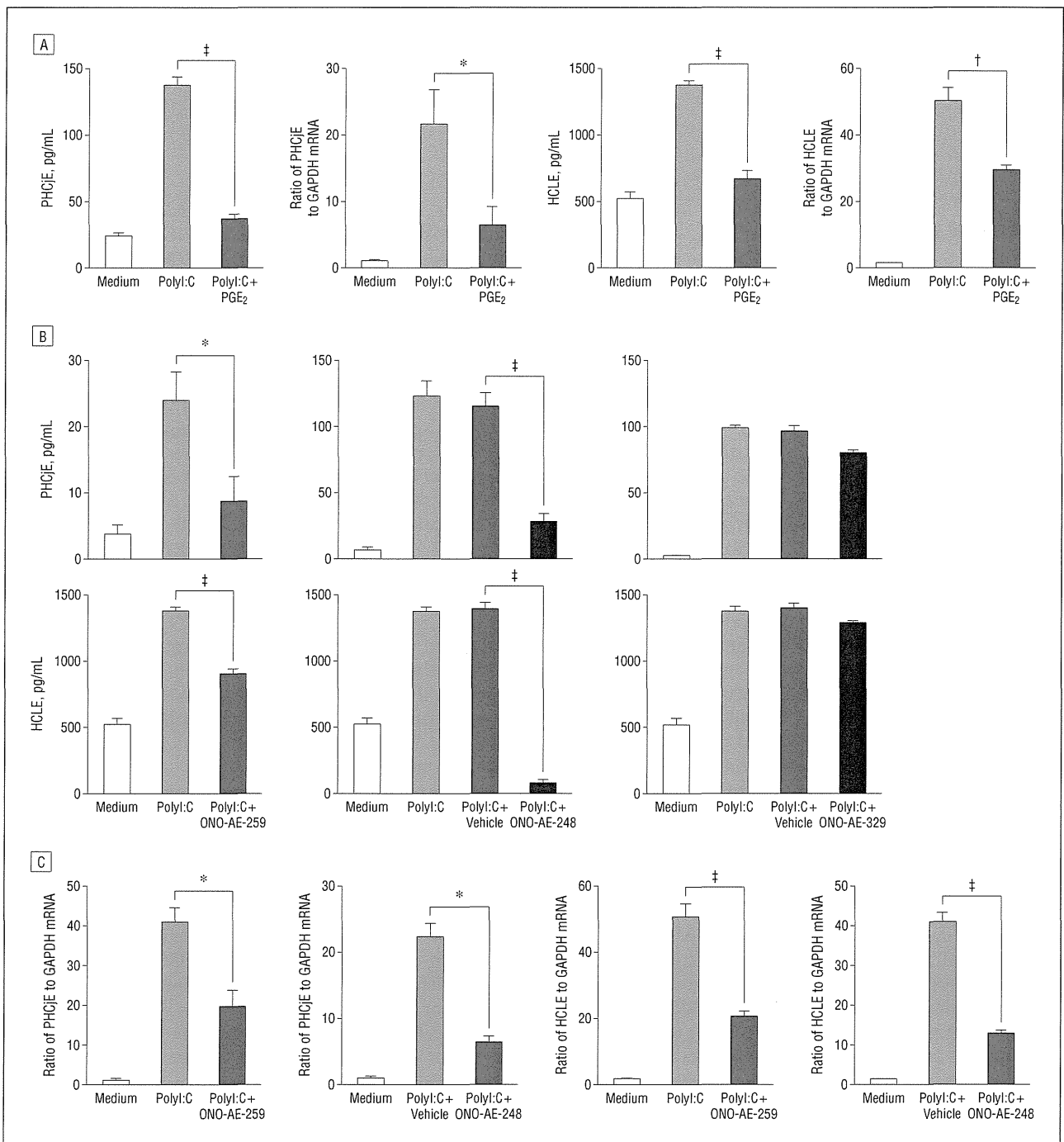


Figure. Prostaglandin E₂ (PGE₂) attenuated the messenger RNA (mRNA) expression and production of monocyte chemoattractant protein 1 via both prostaglandin E receptor 2 (EP₂) and EP₃. A, Primary human conjunctival epithelial cells (PHCjE) and human corneal-limbal epithelial cells (HCLE) were exposed to 10 µg/mL of polyinosine–polycytidylic acid (polyI:C) and 100 µg/mL of PGE₂ for 24 hours (enzyme-linked immunosorbent assay) or 6 hours (quantitative real-time polymerase chain reaction). GAPDH indicates glyceraldehyde-3-phosphate dehydrogenase. B and C, The PHCjE and HCLE were exposed to 10 µg/mL of polyI:C and 10 µg/mL of the EP₂, EP₃, or EP₄ agonist for 24 hours (enzyme-linked immunosorbent assay) (B) or 6 hours (quantitative real-time polymerase chain reaction) (C). Data are representative of 3 separate experiments and are given as the mean (SEM) from 1 experiment carried out in 6 to 8 wells (enzyme-linked immunosorbent assay) (B) or 4 to 6 wells (quantitative real-time polymerase chain reaction) (C) per group. **P* < .05; †*P* < .005; ‡*P* < .001.

jiicho, Hirokoji, Kawaramachi, Kamigyoku, Kyoto 602-0841, Japan (mueta@koto.kpu-m.ac.jp).

Author Contributions: Dr Ueta had full access to all of the data in the study and takes responsibility for the integrity of the data and the accuracy of the data analysis.

Financial Disclosure: The work described in this article was carried out in collaboration with Ono Pharmaceutical Co Ltd, who supplied ONO-AE-248 used in this study.

Funding/Support: This work was supported in part by grants-in-aid for scientific research from the Japanese Ministry of Health, Labour, and Welfare, the Japanese Ministry of Education, Culture, Sports, Science, and Technology, the Kyoto Foundation for the Promotion of Medical Science, the National Institute of Biomedical Innovation of Japan, the Intramural Research Fund of Kyoto Prefectural University of Medicine, and the

Shimizu Foundation for Immunological Research Grant.

Online-Only Material: The eAppendix is available at <http://www.archophthalmol.com>.

Additional Contributions: Chikako Endo provided technical assistance.

1. Yagi T, Sotozono C, Tanaka M, et al. Cytokine storm arising on the ocular surface in a patient with Stevens-Johnson syndrome. *Br J Ophthalmol*. 2011; 95(7):1030-1031.
2. Ueta M, Sotozono C, Nakano M, et al. Association between prostaglandin E receptor 3 polymorphisms and Stevens-Johnson syndrome identified by means of a genome-wide association study. *J Allergy Clin Immunol*. 2010;126(6): 1218-1225, e10.
3. Ueta M, Matsuoka T, Yokoi N, Kinoshita S. Prostaglandin E2 suppresses polyinosine-polycytidylic acid (polyI:C)-stimulated cytokine production via prostaglandin E2 receptor (EP) 2 and 3 in human conjunctival epithelial cells. *Br J Ophthalmol*. 2011;95(6):859-863.
4. Ueta M, Matsuoka T, Yokoi N, Kinoshita S. Prostaglandin E receptor subtype EP3 downregulates TSLP expression in human conjunctival epithelium. *Br J Ophthalmol*. 2011;95(5):742-743.
5. Ueta M, Kinoshita S. Innate immunity of the ocular surface. *Brain Res Bull*. 2010;81(2-3):219-228.
6. Takayama K, Garcia-Cardena G, Sukhova GK, Comander J, Gimbrone MA Jr, Libby P. Prostaglandin E2 suppresses chemokine production in human macrophages through the EP4 receptor. *J Biol Chem*. 2002;277(46):44147-44154.

Depth Profile Study of Abnormal Collagen Orientation in Keratoconus Corneas

In a previous study,¹ we used femtosecond laser technology to cut ex vivo human corneas into anterior, mid, and posterior sections, after which x-ray scatter patterns were obtained at fine intervals over each specimen. Data analysis revealed the predominant orientation of collagen at each sampling site, which was assembled to show the variation in collagen orientation between central and peripheral regions of the cornea and as a function of tissue depth. We hypothesized that the predominantly orthogonal arrangement of collagen (directed toward opposing sets of rectus muscles) in the mid and posterior stroma may help to distribute strain in the cornea by allowing it to withstand the pull of the extraocular muscles. It was also suggested that the more isotropic arrangement in the anterior stroma may play a role in tissue biomechanics by resisting intraocular pressure while at the same time maintaining corneal curvature. This article, in conjunction with our findings of abnormal collagen orientation in full-thickness keratoconus corneas,^{2,3} received a great deal of interest from the scientific community and prompted the following question: how does collagen orientation change as a function of tissue depth when the anterior curvature of the cornea is abnormal, as in keratoconus? Herein, we report findings from our investigation aimed at answering this question.

Methods. The Baron chamber used in our previous study¹ was adapted to enable corneal buttons to be clamped in place and inflated (by pumping physiological saline into the posterior compartment) to restore their natural curvature. A button diameter of 8 mm or larger was deemed necessary to ensure tissue stability during this process.

The next step, obtaining fresh, full-thickness, keratoconus buttons of sufficient diameter, proved to be problematic owing to the increasing popularity of deep anterior lamellar keratoplasty. Recently, however, the

opportunity arose to examine an 8-mm full-thickness (300-340 μm minus epithelium) keratoconus corneal button with some central scarring and a mean power greater than 51.8 diopters (**Figure 1**). The tissue was obtained in accordance with the tenets of the Declaration of Helsinki and with full informed consent from a 31-year-old patient at the time of penetrating keratoplasty. Using techniques detailed previously,¹ the corneal button was clamped in the chamber and inflated. The central 6.3-mm region of the button was then flattened by the applanation cone and a single cut was made at a depth of 150 μm from the surface using an IntraLase 60-kHz femtosecond laser (Abbott Medical Optics Inc),¹ thus splitting the cornea into anterior and posterior sections of roughly equal thickness. Wide-angle x-ray scattering patterns were collected at 0.25-mm intervals over each cor-

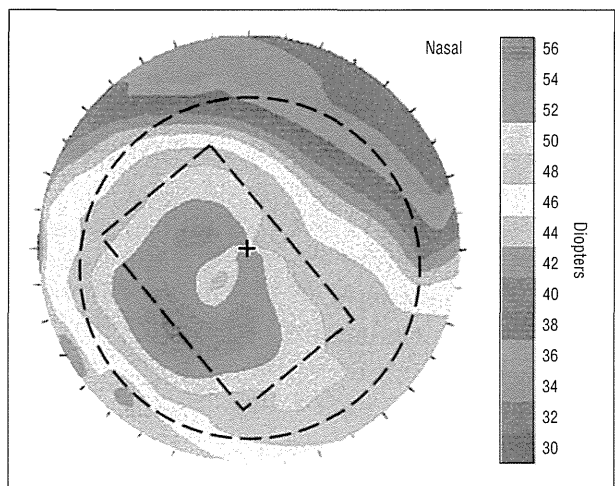


Figure 1. Corneal topography of the keratoconus cornea (recorded 12 years previously).³ The broken lines show the 6.3-mm region of the cornea cut with the femtosecond laser (circle) and the region of greatest corneal steepening depicted in Figure 2 (rectangle).

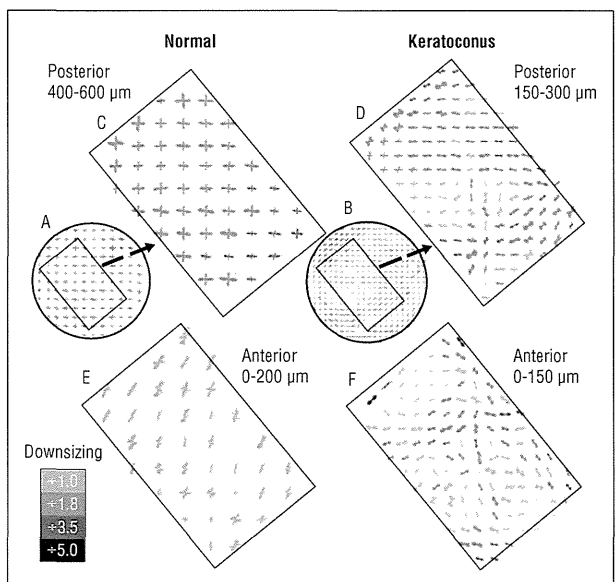


Figure 2. Collagen orientation in the normal (A) and keratoconus (B) posterior stroma (central 6.3 mm). The highlighted regions of the posterior (C and D) and anterior (E and F) stroma are expanded. Large vector plots showing high collagen alignment are downsized (key).